Square superlattice pattern in dielectric barrier discharge

Lifang Dong,* Weili Fan, Yafeng He, Fucheng Liu, Shufeng Li, Ruiling Gao, and Long Wang
College of Physics Science & Technology, Hebei University, Baoding, 071002, China
(Received 9 January 2006; published 6 June 2006)

We report the observation of a square superlattice pattern in a dielectric barrier discharge system. The correlation measurements indicate that the square superlattice pattern is an interleaving of two different transient square sublattices. The interplay between the charge pattern and the discharge filament pattern is discussed.

DOI: 10.1103/PhysRevE.73.066206 PACS number(s): 47.54.−r, 52.80.Tn, 89.75.Kd

A superlattice pattern is a spatially periodic, sometimes strikingly complex, structure composed of two or more simple planforms. In biology, natural superlattices are familiar, such as fish skins [1] and morphogenetic phenomena [2]. In addition, patterns of alternating large and small spots are also common, for example, the scale patterns on the head of the lizard *Cyrtodactylus fedtschenkoi* [3]. Superlattice patterns can be studied in laboratory experiments, such as Faraday experiment [4], reaction-diffusion [5,6], hydrodynamic [7], magnetohydrodynamic [8], and nonlinear optics [9]. In general, more intricate methods are applied to produce superlattice patterns in the above systems. In a "Faraday experiment," two frequency forcing is utilized, in which the time translation symmetry is broken by introducing a second perturbing frequency component [4]. In a photosensitive reaction-diffusion system, a brief spatially periodic forcing is needed [5]. In a nonlinear optical system, a controllable phase-only spatial Fourier filter is placed in the system's diffractive feedback loop [9], and in hydrodynamics both a vertical temperature difference and vertical time-periodic oscillations are imposed on the fluid layer [7]. Some theoretical efforts on the superlattice formation mechanism have been devoted [3,10,11]. Patterns consisting of large and small spots were simulated in a reaction-diffusion system with spatially varying parameters [3].

In this paper, we report the observation of a square superlattice pattern composed of large and small spots, as shown in Fig. 1, in dielectric barrier discharge (DBD) by applying only one frequency forcing. The spatial-temporal dynamics of the square superlattice pattern is studied by correlation measurements. The interplay between the charge pattern and the discharge filament pattern is also discussed.

The experimental device is shown in Fig. 2. Two cylindrical containers, with diameters of 65 mm, sealed with 1.5 mm thick glass plates are filled with water. There is a metallic ring immersed in each of the containers and connected to a power supply. Thus, the water acts as a liquid electrode. The glass plates serve as dielectric layers. A glass frame with the thickness of 1.6 mm was placed between the two parallel glass plates, serving as the lateral boundary. A sinusoidal ac voltage is applied to the electrodes. All of the apparatus are enclosed in a big container filled with argon. The gas pressure is kept at atmospheric pressure. The amplitude of the applied voltage is measured by a high-voltage probe (Tektronix P6015A 1000X). The light emitted from two individual discharge filaments is detected by two lens-aperture-photomultiplier tube (PMTs, RCA 7265) systems and recorded with an oscilloscope (Tektronix TDS3054B, 500 MHz) simultaneously. Thus the correlation between two discharge filaments can be studied [12,13].

It is found that the square superlattice pattern can be observed in rectangular and square boundary conditions as shown in Fig. 1. Figure 3 displays the bifurcation scenario of the patterns when the applied voltage is increased, which follows as the square pattern [12]–quasisuperlattice–square superlattice pattern–hexagon pattern. Figure 4 shows a phase diagram of these emerging patterns. The square superlattice pattern appears in the frequency range from 45 to 80 kHz and the voltage range from 3.6 to 4.4 kV.

Figure 5 gives the wave forms of the total light of the patterns shown in Fig. 3. There are two discharge pulses in each half cycle of the applied voltage for the square pattern, while three for the square superlattice pattern. Similar one-dimensional DBD patterns, from the point of view of the number of discharge stages and the filament size, were observed [14].

Figure 1 shows the time-average square superlattice patterns over thousands of driving cycles. In order to know the spatiotemporal behavior of the square superlattice pattern in time scales shorter than the half driving cycle, the temporal correlations between individual discharge filaments are measured and shown in Fig. 6. It is found that not all of the spots are ignited simultaneously [Fig. 6(a)], whereas all of the small spots volley at the rising edge of the voltage [Fig. 6(b)]

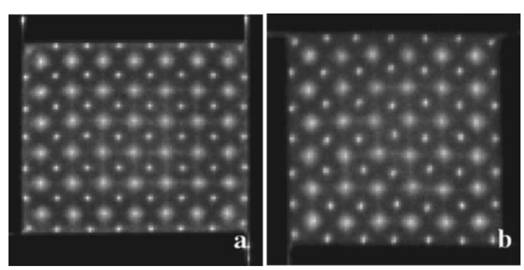

FIG. 1. Square superlattice patterns observed in DBD in (a) a rectangular boundary and (b) a square boundary. The applied voltage $U=4.2$ kV. The driven frequency $f=62$ kHz. The exposure time of the image is 40 ms. The size of the discharge area is 37.2×32.5 mm in (a), and 32.5×32.5 mm in (b).

*Electronic address: Donglf@mail.hbu.edu.cn

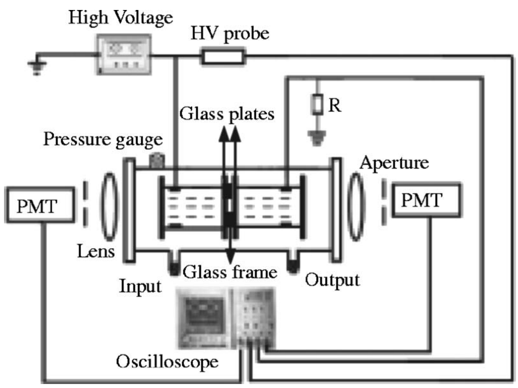

FIG. 2. Schematic diagram of the experimental setup.

and all of the large spots are ignited synchronously two times [Fig. 6(c)], one at the rising edge and the other at the falling edge in each half cycle of applied voltage, though there are some fluctuations in discharge. So the square superlattice pattern is a spatiotemporal pattern resulting from an interleaving of two transient square sublattices—the small-spot square sublattice (denoted by S) and the large-spot square sublattice (denoted by L). The temporal evolution of the square superlattice pattern is shown schematically in the right column in Fig. 7. In each half cycle of the applied voltage, S appears once while L appears twice. The sequence of two transient sublattices is S-L-L-S-L-L in one cycle of the voltage, which is different from that in the square pattern [see Fig. 3(a)]. As studied previously [12], the square pattern is an interleaving of two equivalent square sublattices (denoted by s and l) with the sequence of s-l-l-s in each cycle of the voltage, which has a sequence inversion. However, such an inversion disappears in the square superlattice pattern. To some extent, it can be said that the spatial translation symmetry is lowered but the temporal translation symmetry becomes higher when the square pattern bifurcates to a square superlattice pattern. The key to this symmetry transition is the second ignition of the large spots at the falling edge resulting from the increase of the wall charge density.

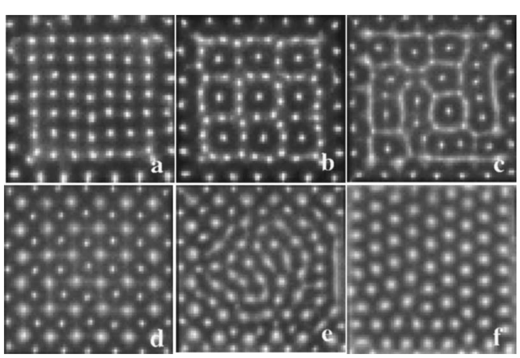

FIG. 3. Pattern scenario with the increase of applied voltage. (a) square pattern, $U=3.2$ kV, (b) quasisuperlattice pattern, $U=3.5$ kV, (c) the prepattern of the square superlattice, $U=3.8$ kV, (d) square superlattice pattern, $U=4.2$ kV, (e) destabilization of the square superlattice $U=4.3$ kV, and (f) hexagon pattern $U=5.0$ kV. The exposure time of the image is 40 ms. The original size of each picture is 32.5×32.5 mm. $f=62$ kHz.

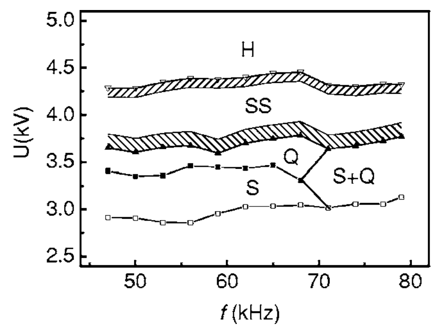

FIG. 4. Phase diagram of the pattern types as a function of the applied voltage U and the driven frequency f. S, square pattern; Q, quasisuperlattice pattern; SS, square superlattice pattern; H, hexagon pattern; $S+Q$, coexistence of the square pattern and quasisuperlattice pattern. The marked strips indicate the regions of prepattern and destabilization of the square superlattice pattern, repectively.

As well known, the charges created in a filament accumulate on the surface of the dielectric layer, which are called wall charges [15,16]. They will set up a field $[E(Q)]$ opposite to the present applied field, which extinguishes this discharge. The higher the voltage is at the discharge moment, the higher wall charge density is needed to extinguish this discharge. Thus the charge density in large spots could be bigger than that of the small spot after the discharge at the rising edge of applied voltage. However the field $E(Q)$ will aid the next discharge at the same position. If $E(Q)$ is lower than the breakdown field threshold, the next discharge will occur at the rising edge when the applied voltage changes the polarity [12]. The wall charges will change sign from Q to $-Q'$ after discharge. Any discharge at the rising edge of applied voltage belongs to this case. If $E(Q)$ is higher than the breakdown field threshold, the next discharge will occur at the falling edge in this half cycle [17]. The wall charge density will be reduced but the sign of charges is not changed. The ignition of the large spot at the falling edge belongs to this case.

Generally, wall charges are localized at the positions of filaments due to the slow mobility on the insulator surface,

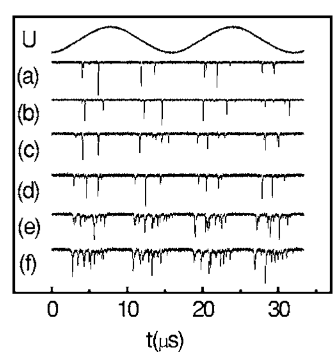

FIG. 5. The wave forms of the total light of the square pattern (a), the quasisuperlattice pattern (b), the prepattern of the square superlattice (c), the square superlattice pattern (d), the destabilization of a square superlattice (e), and the hexagon (f). The top curve is the wave form of the applied voltage.

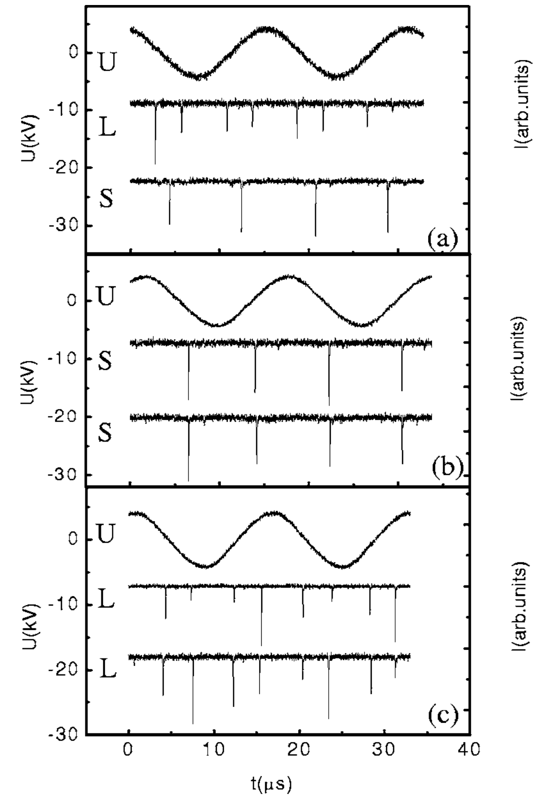

FIG. 6. Temporal correlations between two spots (filaments) in a square superlattice pattern (U=4.2 kV, f=62 kHz.) (a) a large spot and a small spot, (b) two small spots, and (c) two large spots. L stands for a large spot and S stands for a small spot.

leading to the existence of a charge pattern on the dielectric surface. They will set up a transversely nonuniform charge pattern field. The net field imposed on gas, which is the combination of the charge pattern field and the external field, is therefore transversely nonuniform. The filaments are ignited where the net field reaches the breakdown field threshold. Thus the charge pattern, as a spatially varying forcing, determines the positions and the moments of the discharge. Inversely, the charge pattern is rearranged by the accumulating charges during the discharge. At a certain voltage there should exist a self-consistent state that the steady regular pattern is self-organized.

Figure 7 illustrates schematically the interplay of the charge pattern on a dielectric surface and discharge filament pattern in the square superlattice pattern. In region I, the negative wall charge density in small spots is higher than that of large spots, leading to the small-spot filament pattern $1(S)$ at first at the rising edge of applied voltage. The wall charges in small spots become positive after discharge (see the charge pattern in region II). A further increase of the applied voltage leads to the ignition of the large-spot filament pattern $2(L)$. Much more positive charges are then created (see the charge pattern in region III), which initiates a second large-spot filament pattern $3(L)$ at the falling edge resulting in the reduction of the wall charge density. The evolution of the charge pattern and the discharge filament pattern in IV$-4(S)-$V$-5(L)-$VI$-6(L)$ is similar to that described above only by changing the sign of the charges. The charge pattern after the discharge pulse $6(L)$ will become the charge pattern in region I once again.

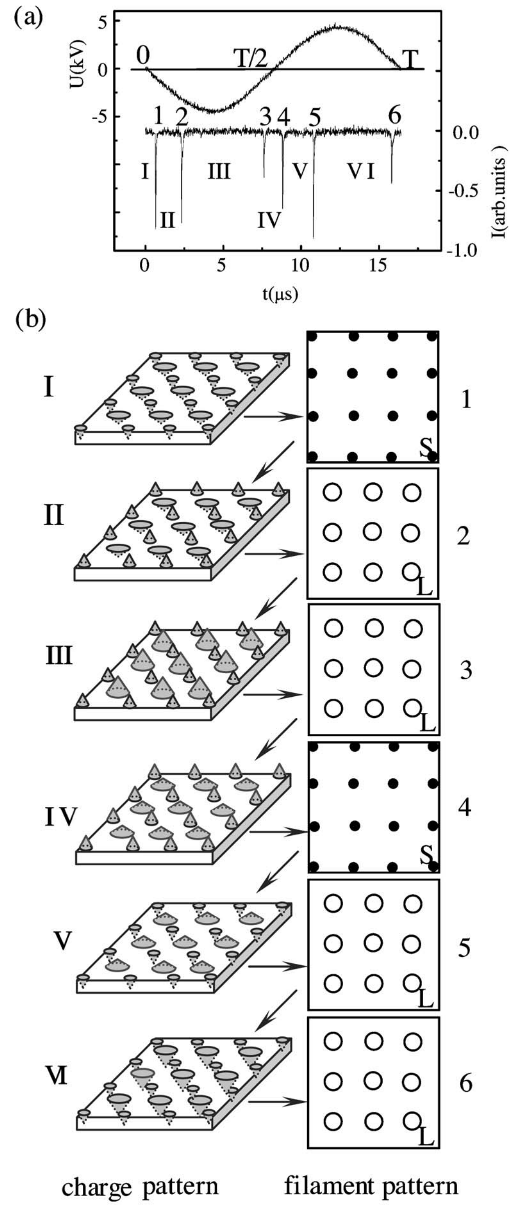

FIG. 7. Schematic diagram of the interplay between a charge pattern and a discharge filament pattern. (a) The wave forms of the applied voltage in one driving cycle and the total light of a large spot and a small spot. (b) A sketch of temporal evolution of the charge patterns and the discharge patterns in time sequence I-1–II-2–III-3–IV-4–V-5–VI-6 denoted in (a). The variations of charge patterns in pulses 1–6 are very rapid and not shown here. The arrows indicate the time sequence. The cone stands for negative charges while the inverted cone stands for positive. The higher the symbol is, the bigger the charge density is.

In conclusion, the square superlattice pattern is observed in a gas discharge system. The spatial-temporal dynamics of the square superlattice pattern is studied by correlation measurements. It is found that the square superlattice pattern is an interleaving of two different transient square sublattices.

The interplay between the charge pattern and the discharge filament pattern is also discussed.

This work was supported by the National Natural Science Foundation of China under Grants No. 10575027 and No. 10375015, the Specialized Research Fund for the Doctoral Program of higher Education of China (Grant No. 20050075001), and the Natural Science Foundation of Hebei Province, China under Grants No. A2004000086 and No. A2006000950.

[1] R. A. Barrio, C. Varea, J. L. Aragon, and P. K. Maini, Bull. Math. Biol. **61**, 483 (1999).
[2] P. K. Maini, K. J. Painter, and H. N. P. Chau, J. Chem. Soc., Faraday Trans. **93**, 3601 (1999).
[3] K. M. Page, P. K. Maini, and N. A. M. Monk, Physica D **202**, 95 (2005).
[4] M. Silber, C. M. Topaz, and A. C. Skeldon, Physica D **143**, 205 (2000); A. Kudrolli, B. Pier, and J. P. Gollub, *ibid.* **123**, 99 (1998).
[5] I. Berenstein, L. Yang, M. Dolnik, A. M. Zhabotinsky, and I. R. Epstein, Phys. Rev. Lett. **91**, 058302 (2003).
[6] L. Yang, M. Dolnik, A. M. Zhabotinsky, and I. R. Epstein, Phys. Rev. Lett. **88**, 208303 (2002).
[7] J. L. Rogers, M. F. Schatz, O. Brausch, and W. Pesch, Phys. Rev. Lett. **85**, 4281 (2000); H. Arbell and J. Fineberg, *ibid.* **81**, 4384 (1998).
[8] H. J. Pi, S. Y. Park, J. Lee, and K. J. Lee, Phys. Rev. Lett. **84**, 5316 (2000).
[9] M. A. Vorontsov and B. A. Samson, Phys. Rev. A **57**, 3040 (1998).
[10] S. L. Judd and M. Silber, Physica D **136**, 45 (2000).
[11] C. M. Topaz, J. Porter, and M. Silber, Phys. Rev. E **70**, 066206 (2004).
[12] L. F. Dong, Z. Q. Yin, L. Wang, G. S. Fu, Y. F. He, Z. F. Chai, and X. C. Li, Thin Solid Films **435**, 120 (2003).
[13] L. F. Dong, F. C. Liu, S. H. Liu, Y. F. He, and W. L. Fan, Phys. Rev. E **72**, 046215 (2005).
[14] J. Guikema, N. Miller, J. Niehof, M. Klein, and M. Walhout, Phys. Rev. Lett. **85**, 3817 (2000); M. Klein, N. Miller, and M. Walhout, Phys. Rev. E **64**, 026402 (2001).
[15] W. Breazeal, K. M. Flynn, and E. G. Gwinn, Phys. Rev. E **52**, 1503 (1995).
[16] I. Brauer, C. Punset, H.-G. Purwins, and J. P. Boeuf, J. Appl. Phys. **85**, 7569 (1999).
[17] L. F. Dong, Z. G. Mao, Z. Q. Yin, and J. X. Ran, Appl. Phys. Lett. **84**, 5142 (2004).